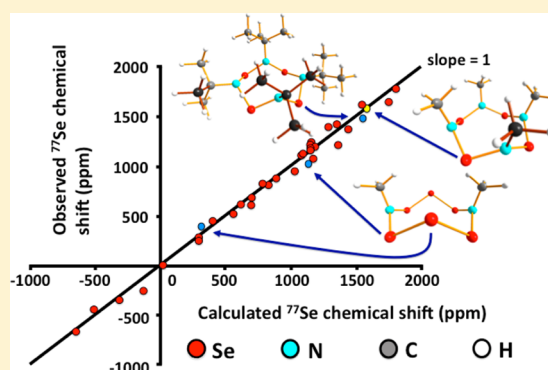


Experimental and Computational ^{77}Se NMR Investigations of the Cyclic Eight-Membered Selenium Imides $1,3,5,7\text{-Se}_4(\text{NR})_4$ ($\text{R} = \text{Me}$, ^tBu) and $1,5\text{-Se}_6(\text{NMe})_2$ Aino J. Karhu,[†] Olli J. Pakkanen,[†] J. Mikko Rautiainen,[†] Raija Oilunkaniemi,[†] Tristram Chivers,[‡] and Risto S. Laitinen^{*,†}[†]Laboratory of Inorganic Chemistry, Center for Molecular Materials, University of Oulu, P.O. Box 3000, Oulu FI-90014, Finland[‡]Department of Chemistry, University of Calgary, 2500 University Drive, N.W., Calgary, Alberta T2N 1N4, Canada

Supporting Information

ABSTRACT: The cyclocondensation reaction of equimolar amounts of SeCl_2 and $(\text{Me}_3\text{Si})_2\text{NMe}$ in THF affords $1,3,5,7\text{-Se}_4(\text{NMe})_4$ (**5b**) [$\delta(^{77}\text{Se}) = 1585$ ppm] in excellent yield. An X-ray structural determination showed that **5b** consists of cyclic, puckered crown-shaped molecules with a mean Se–N bond length of 1.841 Å typical of single bonds. A minor product of this reaction was isolated as unstable orange-red crystals, which were identified by X-ray analysis as the adduct $1,5\text{-Se}_6(\text{NMe})_2 \cdot \frac{1}{2}\text{Se}_8$ (**1b**· $\frac{1}{2}\text{Se}_8$), composed of cyclic $1,5\text{-Se}_6(\text{NMe})_2$ and disordered *cyclo*- Se_8 molecules. A detailed reinvestigation of the cyclocondensation reaction of SeCl_2 and $^t\text{BuNH}_2$ as a function of molar ratio and time by multinuclear (^1H , ^{13}C , and ^{77}Se) NMR spectroscopy revealed that the final product exhibits one ^{77}Se resonance at 1486 ppm and equivalent ^tBu groups. The shielding tensors of 28 selenium-containing molecules, for which the ^{77}Se chemical shifts are unambiguously known, were calculated at the PBE0/def2-TZVPP level of theory to assist the spectral assignment of new cyclic selenium imides. The good agreement between the observed and calculated chemical shifts enabled the assignment of the resonance at 1486 ppm to $1,3,5,7\text{-Se}_4(\text{N}^t\text{Bu})_4$ (**5a**). Those at 1028 and 399 ppm (intensity ratio 2:1) could be attributed to $1,5\text{-Se}_6(\text{NMe})_2$ (**1b**).



INTRODUCTION

Sulfur has long been known to form a series of eight-membered cyclic imides $\text{S}_{8-n}(\text{NH})_n$ ($n = 1-4$), the structures of which are well-established.¹ The best-known example is $\text{S}_4(\text{NH})_4$,² which also forms a 2:1 sandwich complex in which all four sulfur atoms are bonded to Ag^+ ions,^{3a} but behaves as a S-monodentate ligand in complexes of the type $\text{S}_4(\text{NH})_4\text{M}(\text{CO})_5$ ($\text{M} = \text{Cr}, \text{W}$).^{3b} Cyclic organic derivatives, e.g., $1,4\text{-S}_4(\text{NR})_2$ ($\text{R} = \text{Et}, \text{Bz}, \text{Cy}, \text{CH}_2\text{CH}_2\text{Ph}$)^{4a} and $1,3,5,7\text{-S}_4(\text{NMe})_4$ ^{4b} are obtained via cyclocondensation of the appropriate primary amine and SCl_2 or S_2Cl_2 .

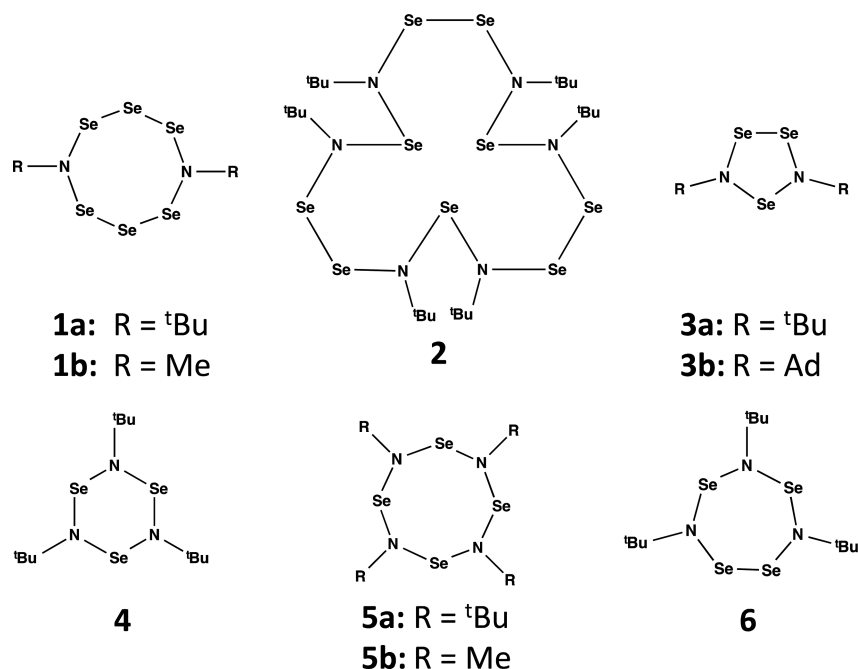
In contrast to the long and venerable history of cyclic sulfur imides,^{1d} the development of the chemistry of cyclic selenium imides has been slow. The parent imides have not been reported, but several organic derivatives have been prepared and structurally characterized (see Chart 1). Roesky and Bats⁵ pioneered this field with their report of the synthesis and crystal structures of the eight-membered ring $1,5\text{-Se}_6(\text{N}^t\text{Bu})_2$ (**1a**) and the 15-membered ring $1,3,6,8,11,13\text{-Se}_9(\text{N}^t\text{Bu})_6$ (**2**), which were both obtained from reactions of $(^t\text{Bu})(\text{Me}_3\text{Si})\text{NLi}$ with Se_2Cl_2 and SeOCl_2 . Subsequently, Herberhold and Jellen⁶ utilized the reaction of the same lithiated reagent with SeCl_4 and deduced the formation of the five-membered ring $1,3\text{-Se}_3(\text{N}^t\text{Bu})_2$ (**3a**) by NMR spectroscopy. The best yields of **1a** and **2** (11% and 64%, respectively) are obtained by the treatment of $^t\text{BuNH}_2$ with an equimolar mixture of SeCl_4 and elemental selenium in THF.⁷ The cyclocondensation reaction of $^t\text{BuNH}_2$ and SeCl_2 , prepared *in situ* by the reaction of elemental selenium and SO_2Cl_2 in THF,⁸ yields a complicated mixture from which the cyclic selenium imides **1a**, **2**, **3a**, and $1,3,5\text{-Se}_3(\text{N}^t\text{Bu})_3$ (**4**), as well as the hydrolysis products $^t\text{BuNSe}(\mu\text{-N}^t\text{Bu})_2\text{SeO}$ and $^t\text{BuNSe}(\mu\text{-N}^t\text{Bu})_2\text{SO}_2$, and the acyclic imidoselenium dichlorides $\text{ClSe}[\text{N}(\text{N}^t\text{Bu})\text{Se}]_n\text{Cl}$ ($n = 1, 2$), were isolated and characterized.^{7,9} The use of adamantylamine AdNH_2 in the cyclocondensation reaction produced a similar mixture from which the five-membered ring $1,3\text{-Se}_3(\text{NAd})_2$ (**3b**) was isolated in good yields and structurally characterized.¹⁰

We have recently observed that the reaction of *tert*-butyl selenium diimide, $\text{Se}(\text{N}^t\text{Bu})_2$, with $[\text{PdCl}_2(\text{NCPH})_2]$ affords the complexes $[\text{PdCl}_2\{\text{Se}, \text{Se}'\text{-Se}_4(\text{N}^t\text{Bu})_4\}]$ and $[\text{PdCl}_2\{\text{Se}, \text{Se}'\text{-Se}_4(\text{N}^t\text{Bu})_3\}]$, which contain cyclic $1,3,5,7\text{-Se}_4(\text{N}^t\text{Bu})_4$ (**5a**) and $1,3,5\text{-Se}_4(\text{N}^t\text{Bu})_3$ (**6**) ligands, respectively.¹¹ However, the

Received: March 17, 2015

Published: May 1, 2015

Chart 1



isolation and characterization of free **5a** and **6** has thus far not been possible. Interestingly, the ^{77}Se NMR spectrum of the solution from the reaction of $^t\text{BuNH}_2$ and SeCl_2 exhibited a strong resonance at 1486 ppm,⁷ which has been tentatively attributed to 1,3,5,7- $\text{Se}_4(\text{N}^t\text{Bu})_4$ (**5a**).^{11,12}

In the light of these recent findings we have focused our attention on the development of a new method for the synthesis of cyclic selenium imides, notably the eight-membered ring **5b**, 1,3,5,7- $\text{Se}_4(\text{NMe})_4$. The preparation of the sulfur analogue of **5b** by the cyclocondensation of methylamine and SCl_2 in hexane required a laborious procedure in order to separate $\text{S}_4(\text{NMe})_4$ from the other products, including insoluble $(\text{MeNH}_3)\text{Cl}$.^{4b} The reaction of $^t\text{BuNH}_2$ and SeCl_2 in THF suffers from a similar disadvantage owing to the formation of copious amounts of $(^t\text{BuNH}_3)\text{Cl}$.⁷ In order to circumvent this problem we have employed the commercially available reagent $(\text{Me}_3\text{Si})_2\text{NMe}$ in reactions with *in situ* generated SeCl_2 , since the condensation product Me_3SiCl is easily removed under vacuum. In this article, we report the high-yield synthesis of 1,3,5,7- $\text{Se}_4(\text{NMe})_4$ (**5b**) via this approach together with the multinuclear NMR spectra and X-ray crystal structure of this new cyclic selenium imide. An unstable, orange-red minor product was also isolated and identified by an X-ray analysis as the adduct 1,5- $\text{Se}_6(\text{NMe})_2 \cdot \frac{1}{2}\text{Se}_8$ (**1b** $\cdot\frac{1}{2}\text{Se}_8$). DFT calculations of the ^{77}Se NMR chemical shifts of 28 compounds for which experimental data are available were utilized for the assignment of ^{77}Se NMR resonances to 1,3,5,7- $\text{Se}_4(\text{N}^t\text{Bu})_4$ (**5a**) and 1,5- $\text{Se}_6(\text{NMe})_2$ (**1b**).

EXPERIMENTAL SECTION

General Procedures. All manipulations involving air- and moisture-sensitive materials were conducted under an argon atmosphere by using Schlenk techniques or in a drybox. Tetrahydrofuran and *n*-hexane were distilled over Na/benzophenone under an argon atmosphere prior to use. Selenium granules (Merck), SO_2Cl_2 (Aldrich), and $(\text{Me}_3\text{Si})_2\text{NMe}$ (Fluka) were used without further purification. SeCl_2 was prepared from freshly ground selenium and

SO_2Cl_2 in THF by the literature procedure.⁸ The reaction of $^t\text{BuNH}_2$ and SeCl_2 was carried out, as described previously,⁷ but the molar ratios of the reactants were varied and the reactions were monitored by ^{77}Se NMR spectroscopy over an extended period of time.

NMR Spectroscopy. ^1H , ^{13}C , and ^{77}Se NMR spectra were recorded in C_7D_8 on a Bruker Avance III 400 spectrometer operating at 400.13, 100.62, and 76.31 MHz, respectively. Typical respective spectral widths were 8.22, 24.04, and 113.64 kHz, and the pulse widths were 26.50, 14.30, and 16.75 μs . The pulse delays for proton, carbon, and selenium were 1.0, 2.0, and 1.0 s, respectively. The ^1H and ^{13}C NMR spectra were referenced to the solvent resonances and are reported relative to Me_4Si . The ^{77}Se NMR spectra were referenced externally to a saturated aqueous solution of selenium dioxide. The chemical shifts are reported relative to neat Me_2Se [$\delta(\text{Me}_2\text{Se}) = \delta(\text{SeO}_2) + 1302.6$].¹³

Preparation of 1,3,5,7- $\text{Se}_4(\text{NMe})_4$ (5b**).** A solution of SeCl_2 (10.0 mmol) in THF (5 mL) was added to a solution of $(\text{Me}_3\text{Si})_2\text{NMe}$ (2.2 mL, 10.0 mmol) in THF (20 mL) at -80°C . The reaction mixture was stirred for 30 min at -80°C and further for 1.5 h at -10°C during which time a yellow solution and a yellow precipitate were formed. The solvent and Me_3SiCl byproduct were removed under vacuum to yield **5b** as a solid (0.985 g, 91%). Yellow crystals suitable for the X-ray structure determination were obtained by recrystallization from *n*-hexane at -20°C . Anal. Calcd for $\text{C}_4\text{H}_{12}\text{N}_4\text{Se}_4$: C, 11.12; H, 2.80; N, 12.97%. Found: C, 11.15; H, 2.66; N, 12.25. NMR: δ ^1H (C_7D_8 , 25 $^\circ\text{C}$): 3.85; δ ^{13}C (C_7D_8 , 25 $^\circ\text{C}$): 62.34 (q), $^1J_{\text{HC}}$ 136.84 Hz; δ ^{77}Se (C_7D_8 , 25 $^\circ\text{C}$): 1585.

Formation of 1,5- $\text{Se}_6(\text{NMe})_2 \cdot \frac{1}{2}\text{Se}_8$ (1b** $\cdot\frac{1}{2}\text{Se}_8$).** In a smaller scale reaction a solution of SeCl_2 (2.6 mmol) in THF (3 mL) was added to a solution of $(\text{Me}_3\text{Si})_2\text{NMe}$ (0.57 mL, 2.6 mmol) in THF (10 mL) in a fashion similar to that described above. The yellow precipitate was allowed to settle, and the solution was decanted through a cannula. The solution was concentrated to a volume of ca. 5 mL and stored for three months at -20°C . Several weak ^{77}Se NMR signals appeared in the NMR spectrum during this time, and a small crop of extremely air-sensitive orange-red crystals of 1,5- $\text{Se}_6(\text{NMe})_2 \cdot \frac{1}{2}\text{Se}_8$ (**1b** $\cdot\frac{1}{2}\text{Se}_8$) were formed. ^{77}Se NMR (THF, 25 $^\circ\text{C}$): δ 1028, 399 (intensity ratio 2:1; see below for the assignment).

X-ray Crystallography. The crystals of **5b** and **1b** $\cdot\frac{1}{2}\text{Se}_8$ were coated with Paratone oil and mounted in a nylon CryoLoop, and the diffraction data were collected on a Bruker Nonius Kappa CCD diffractometer at 150 K using graphite-monochromated $\text{Mo K}\alpha$

radiation ($\lambda = 0.71073 \text{ \AA}$; 55 kV, 25 mA). Crystal data and the details of structure determinations are given in Table 1.

Table 1. Crystal Data and Details of Structure Determination of **5b and **1b**^{1/2}Se₈**

	5b	1b ^{1/2} Se ₈
empirical formula	C ₄ H ₁₂ N ₄ Se ₄	C ₂ H ₆ N ₂ Se ₁₀
fw	432.02	847.69
temp (K)	150	150
cryst syst	monoclinic	monoclinic
space group	<i>P</i> 2 ₁ / <i>n</i>	<i>P</i> 2 ₁ / <i>n</i>
<i>a</i> (Å)	6.372(5)	12.000(2)
<i>b</i> (Å)	12.724(5)	5.6347(11)
<i>c</i> (Å)	14.478(5)	23.631(5)
β (deg)	92.131(5)	90.07(3)
<i>V</i> (Å ³)	1172.1(11)	1597.9(5)
<i>Z</i>	4	4
<i>F</i> (000)	800	1488
<i>D</i> _c (g cm ⁻³)	2.448	3.524
μ (Mo <i>K</i> α) (mm ⁻¹)	12.481	22.822
crystal size (mm ³)	0.30 × 0.10 × 0.05	0.12 × 0.10 × 0.08
indep/obsd reflns ^a	2059/1686	2661/1484
<i>R</i> _{int}	0.1482	0.1529
<i>R</i> 1/ <i>wR</i> 2 [<i>I</i> ≥ 2 σ (<i>I</i>)] ^a	0.0676/0.1765	0.1207/0.2737
<i>R</i> 1/ <i>wR</i> 2 (all data) ^a	0.0799/0.1886	0.1969/0.3149
GOF	1.091	1.085

^a*R*1 = $\sum ||F_o| - |F_c|| / \sum |F_o|$, *wR*2 = $[\sum w(F_o^2 - F_c^2)^2 / \sum wF_o^4]^{1/2}$.

Structures were solved by direct methods using SHELXS-2013 and refined using SHELXL-2013.¹⁴ After the full-matrix least-squares refinement of the non-hydrogen atoms with anisotropic thermal parameters, the hydrogen atoms were placed in calculated positions in the CH₃ groups (C–H = 0.98 Å). In the final refinement the hydrogen atoms were riding with the carbon atoms they were bonded to. The isotropic thermal parameters of the hydrogen atoms were fixed at 1.5 times that of the corresponding carbon atoms. The scattering factors for the neutral atoms were those incorporated with the program.

The crystals of 1,5-Se₆(NMe)₂^{1/2}Se₈ (**1b**^{1/2}Se₈) were extremely unstable and decomposed rapidly during the data collection even at a low temperature. Therefore, only the first part of the data set could be used for the structure determination and structure refinement, and even then the refinement was relatively modest (see Table 1). Furthermore, the Se₈ rings in **1b**^{1/2}Se₈ were found to be disordered in two orientations around the symmetry element. Because of the symmetry constraints, the site occupation factors of the two ring molecules were exactly 0.5.

COMPUTATIONAL DETAILS

The theoretical ⁷⁷Se shielding tensors were computed for 1,3,5,7-Se₄(NMe)₄ (**5b**), 1,5-Se₆(NMe)₂ (**1b**), 1,3,5,7-Se₄(N^tBu)₄ (**5a**), and 28 other small selenium compounds for which the experimental ⁷⁷Se chemical shift data are available^{7,9,10,15} (see Table 1S in Supporting Information).

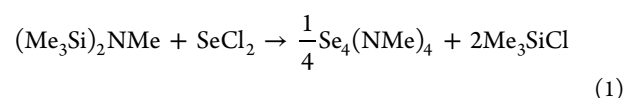
The geometries of all compounds were fully optimized at the DFT level of theory using the PBE0 exchange-correlation hybrid functional¹⁶ effectively reproducing our previous computational approach in the DFT calculation of ⁷⁷Se chemical shifts.¹⁷ The current calculations, however, included Grimme's D3BJ dispersion correction¹⁸ and employed the larger def2-TZVPP basis sets¹⁹ for all atoms. Tight optimization criteria with energy convergence of 10⁻⁷ au and gradient norm convergence of 10⁻⁴ au were imposed to ensure that fully converged geometric parameters are obtained. Molecular parameters from crystal structures of **5b** and **1b**^{1/2}Se₈, as well as relevant selenium-containing molecules determined previously,^{5,7,10,15f,17,20} were used as starting points for geometry optimizations,

and appropriate point group symmetries were utilized in order to speed up calculations. Fundamental vibrations were calculated to establish that the optimized geometries represent local minima.

Nuclear magnetic shielding tensors were calculated for each stationary point employing the GIAO²¹ method, as implemented in the Gaussian 09 software package,²² which was used in all calculations.

RESULTS AND DISCUSSION

Synthesis and NMR Spectra. The cyclocondensation reaction of equimolar amounts of (Me₃Si)₂NMe and SeCl₂ proceeded rapidly (*ca.* 2 h) at -10 °C to afford 1,3,5,7-Se₄(NMe)₄ (**5b**) as a yellow, air-sensitive crystals in over 90% yield (eq 1). As anticipated, the facile removal of the Me₃SiCl byproduct expedited the workup procedure. Unlike previous methods for the synthesis of cyclic selenium imides, (*vide supra*),^{5–7,9,10} this new protocol generates predominantly one product. For comparison, the reactions of (Me₃Si)₂NMe with phosphorus trihalides PX₃ in a 1:1 molar ratio produce the six-membered rings (XPNMe)₃ in 29% (X = Cl) and 74% (X = Br) yields.²³



The ¹H NMR spectrum of **5b** recorded in *d*₈-toluene showed one resonance at 3.85 ppm (¹J_{HC} = 136.84 Hz), and the ¹³C NMR spectrum exhibited a quartet at 62.34 ppm with an identical coupling constant. In the ⁷⁷Se NMR spectrum, a single resonance was observed at 1585 ppm, which is in the 1400–1625 ppm region observed previously for compounds with an NSeN environment.⁷

A very minor product was isolated as thermally unstable, orange-red crystals when the reaction solution was allowed to stand at -20 °C for an extended period. During this time several weak ⁷⁷Se resonances appeared in the solution, and the resonance at 1585 ppm in the ⁷⁷Se NMR spectrum due to **5b** decreased in intensity. Two of the new resonances at 1028 and 399 ppm grew at the constant intensity ratio of 2:1. The previously characterized heterocycle 1,5-Se₆(N^tBu)₂ (**1a**) shows two resonances at 1109 and 518 ppm⁷ suggesting that the current observation may be attributable to the methyl derivative 1,5-Se₆(NMe)₂ (**1b**).

Crystal Structures. The molecular structure of 1,3,5,7-Se₄(NMe)₄ (**5b**) indicating the labeling of atoms is shown in Figure 1. Selected bond lengths and angles are listed in Supporting Information (see Table 2S, see also Figure 3).

The eight-membered ring 1,3,5,7-Se₄(NMe)₄ (**5b**) adopts a puckered, crown-shaped conformation similar to that observed in the sulfur analogues 1,3,5,7-S₄(NMe)₄^{24a} and 1,3,5,7-

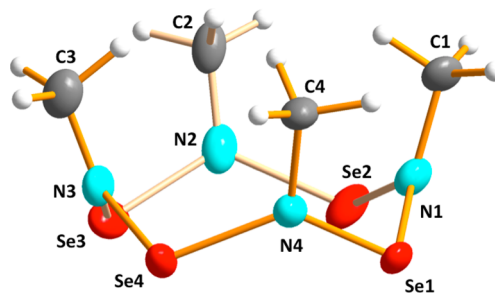


Figure 1. Molecular structure of 1,3,5,7-Se₄(NMe)₄ (**5b**) indicating the labeling of the atoms.

$S_4(NCH_2OH)_4$,^{24b} as well as in the parent imide 1,3,5,7- $S_4(NH)_4$ ² and the adduct 1,3,5,7- $S_4(NH)_4 \cdot 3S_8$.^{25a} By contrast, the 1,3,5,7- $Se_4(N^tBu)_4$ ligand in the palladium(II) complex $[PdCl_2\{Se,Se'-5a\}]$ shows a chair-conformation as a consequence of 1,5- Se,Se' coordination.¹¹

The molecular structure of 1,5- $Se_6(NMe)_2 \cdot \frac{1}{2}Se_8$ (**1b**^{1/2} Se_8) indicating the labeling of atoms is shown in Figure 2. The

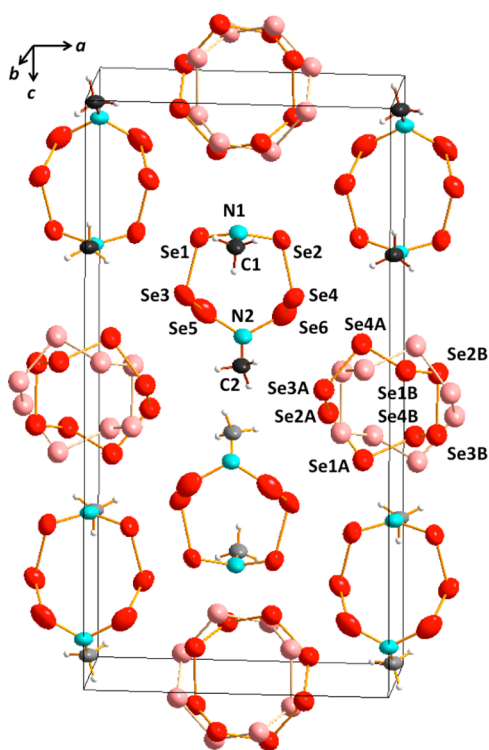


Figure 2. Molecular structure of 1,5- $Se_6(NMe)_2 \cdot \frac{1}{2}Se_8$ (**1b**^{1/2} Se_8) indicating the labeling of the atoms.

tentative X-ray analysis of **1b**^{1/2} Se_8 provided an identification of this minor product as the adduct 1,5- $Se_6(NMe)_2 \cdot \frac{1}{2}Se_8$. The structural parameters are listed in Table 2S in Supporting Information (see also Figure 3). The lattice of **1b**^{1/2} Se_8 consists of 1,5- $Se_6(NMe)_2$ and Se_8 molecules with the latter disordered in two different orientations. Similar hybrid lattices have been reported for $S_6(NH)_2 \cdot 2S_8$ ^{25b} and $S_4(NH)_4 \cdot 3S_8$.^{25a} The disordered Se_8 molecules in **1b**^{1/2} Se_8 show the expected puckered crown-shaped conformation, cf., *cyclo- Se_8* .^{20d,26} The 1,5- $Se_6(NMe)_2$ (**1b**) rings also form crowns reminiscent of the congener **1a**.⁵ The similar sizes and shapes of the cyclic E_8 and $E_n(NR)_{8-n}$ ($E = S, Se$) molecules, and the similar chalcogen–chalcogen intermolecular interactions, may well play a role in the formation of mixed lattices.

The Se–N bond lengths in **5b** span a range 1.818(9)–1.872(10) Å (the sum of covalent radii of selenium and nitrogen is 1.87 Å).²⁷ These values are comparable to those reported for other structurally characterized cyclic selenium imides, as shown in Figures 3 and 4. Perhaps the closest comparisons for **5b** are the six-membered ring 1,3,5- $Se_3(N^tBu)_3$ (**4**) [1.825(4), 1.842(4) Å],⁷ which can be considered as a smaller oligomer of **5a**, and the aforementioned palladium complex $[PdCl_2\{Se,Se'-5a\}]$ [1.842(5)–1.886(5) Å].¹¹ The $\angle NSeN$ bond angles of 108.4(4)–110.4(4)° in **5b** are slightly larger than that of **4** [106.6(2)°]⁷ and ca. 6.5° wider than that in the palladium complex. The difference in the conformations

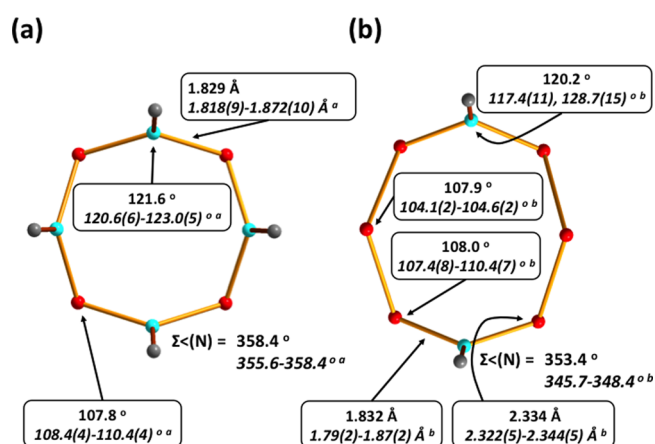


Figure 3. PBE0/def2-TZVPP optimized geometries of (a) 1,3,5,7- $Se_4(NMe)_4$ (**5b**) (molecular symmetry C_{4v}) and (b) 1,5- $Se_6(NMe)_2$ (**1b**) (molecular symmetry C_{2v}) together with the endocyclic bond parameters. The experimental values from the crystal structure determinations are given in italics. *a* indicates **5b** (see Table 2S in Supporting Information). *b* indicates **1b** from the crystal structure of **1b**^{1/2} Se_8 (see Table 2S in Supporting Information).

between **5a** and **5b** due to the coordination of the ring molecule to palladium may have a significant role in case of the latter difference.¹¹ Concomitantly, the $\angle NSeN$ bond angles 120.6(6)–123.0(5)° are ca. 8° wider than those in both **4** and $[PdCl_2\{Se,Se'-5a\}]$.^{7,11}

Optimized Geometries of Cyclic Selenium Imides. The PBE0/def2-TZVPP optimized geometries of 1,3,5,7- $Se_4(NMe)_4$ (**5b**) and 1,5- $Se_6(NMe)_2$ (**1b**) are shown in Figure 3 together with selected calculated endocyclic bond parameters, which are compared to the experimental values from the crystal structure determinations (see Table 2S in Supporting Information).

The corresponding information for the cyclic *tert*-butyl selenium imides 1,3- $Se_3(N^tBu)_2$ (**3a**), 1,3,5- $Se_3(N^tBu)_3$ (**4**), 1,3,5- $Se_4(N^tBu)_3$ (**6**), 1,3,5,7- $Se_4(N^tBu)_4$ (**5a**), 1,5- $Se_6(N^tBu)_2$ (**1a**), and 1,3,6,8,11,13- $Se_9(N^tBu)_6$ (**2**) is shown in Figure 4. It can be seen that the computed geometries in both Figures 3 and 4 predict the experimental structures well. The bond lengths and angles in **5a**, which has only been structurally characterized as a ligand in the palladium complex $[PdCl_2\{Se,Se'-5a\}]$, show reasonable agreement with those predicted for the free **5a** ligand by the DFT calculations. In the complex, however, the ligand exhibits a chair conformation, whereas the free ring system **5a** is expected to be in crown conformation.²⁸ In the case of the seven-membered ring **6**, coordination to palladium in $[PdCl_2\{Se,Se'-6\}]$ does not have a significant effect on the conformation of the ligand.

From an inspection of the data in Figures 3 and 4, it can be seen that the geometry at the nitrogen atoms in cyclic selenium imides is generally close to planar, though there are also deviations. The DFT calculated values, which have been carried out for molecules in a vacuum, predict these deviations well, and therefore they are not only dependent on packing effects in the solid state. The largest deviations from planarity are observed for the strained five-membered ring, 1,3- $Se_3(NAD)_2$ [343.6° and 344.2°;¹⁰ cf., calculated value for 1,3- $Se_3(N^tBu)_2$ (**3a**) of 344.9° and that of 344.7° for 1,3- $Se_3(NAD)_2$ (**3b**)²⁹]. We also note that the lowering of the molecular symmetry from the highest ideal point groups for each cyclic *tert*-butyl selenium imide is a consequence of the relative orientations of the *tert*-

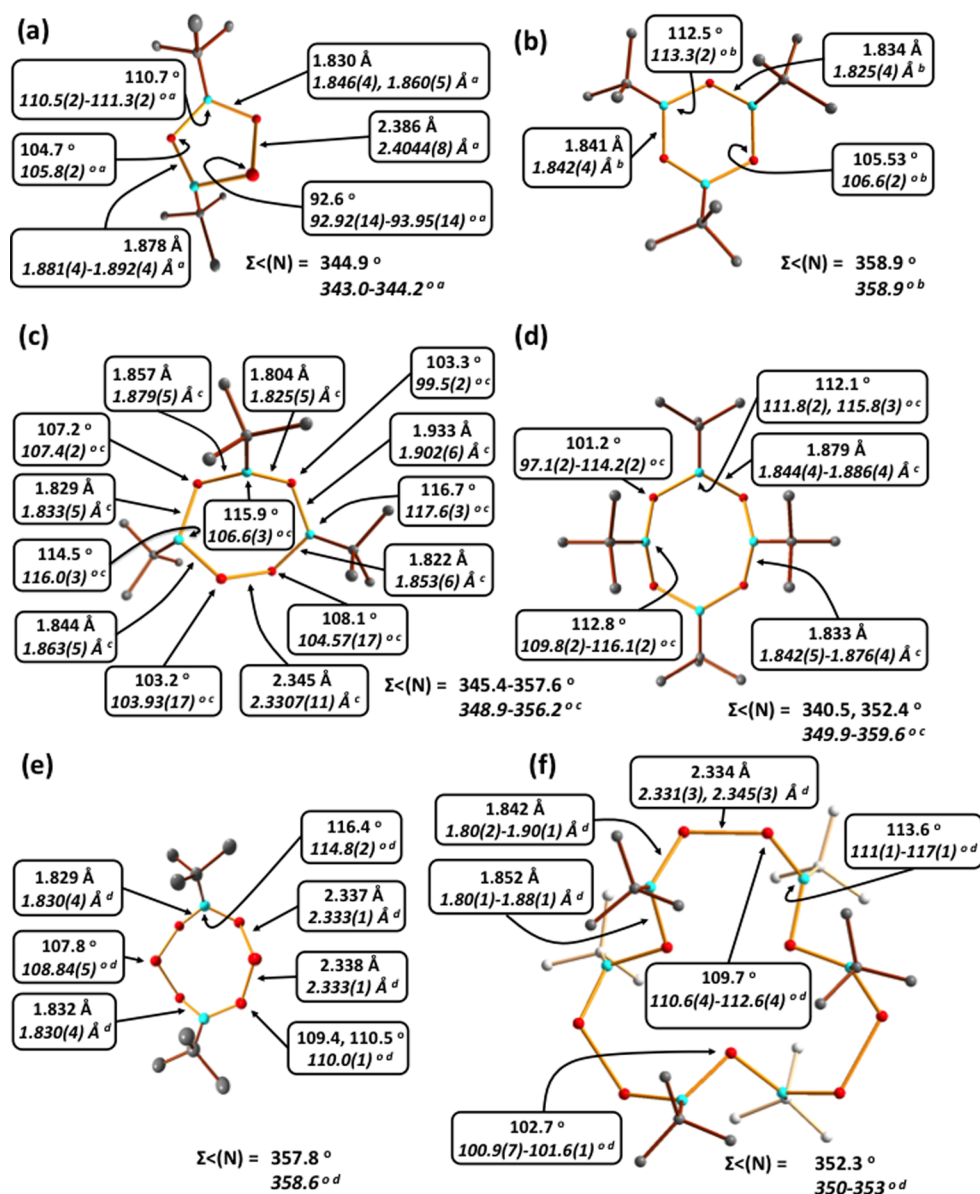


Figure 4. PBE0/def2-TZVPP optimized geometries of (a) 1,3- $\text{Se}_3(\text{N}^t\text{Bu})_2$ (**3a**) (molecular symmetry C_2), (b) 1,3,5- $\text{Se}_3(\text{N}^t\text{Bu})_3$ (**4**) (molecular symmetry C_3), (c) 1,3,5- $\text{Se}_4(\text{N}^t\text{Bu})_3$ (**6**) (molecular symmetry C_1), (d) 1,3,5,7- $\text{Se}_4(\text{N}^t\text{Bu})_4$ (**5a**) (molecular symmetry C_{2v}), (e) 1,5- $\text{Se}_6(\text{N}^t\text{Bu})_2$ (**1a**) (molecular symmetry C_3), and (f) 1,3,6,8,11,13- $\text{Se}_9(\text{N}^t\text{Bu})_6$ (**2**) (molecular symmetry D_3) together with the bond parameters of the ring frameworks. The experimental values from crystal structure determinations are given in italics. *a* indicates 1,3- $\text{Se}_3(\text{NAD})_2$ (**3b**) (ref 10). *b* indicates **4** (ref 7). *c* indicates $[\text{PdCl}_2\{\text{Se}_6\text{Se}'\text{-6}\}]$ and $[\text{PdCl}_2\{\text{Se}_6\text{Se}'\text{-5a}\}]$ (ref 11). *d* indicates **1a** and **2** (ref 5).

butyl groups (see Figure 4). The calculated geometries of the methyl derivatives **1b** and **5b** show the expected highest possible molecular symmetry (see Figure 3).

^{77}Se NMR Chemical Shifts of 1,3,5,7- $\text{Se}_4(\text{NMe})_4$ (5b**) and 1,5- $\text{Se}_6(\text{NMe})_2$ (**1b**).** Accurate theoretical calculations of the ^{77}Se shielding tensors and consequently the chemical shifts require a high level of theory with the consideration of electron correlation, relativistic effects, and solvent effects.³⁰ We have utilized PBE0/def2-TZVPP calculations to obtain absolute shielding tensors σ and their traces σ_{iso} for 28 selected selenium compounds (see Table 1S in Supporting Information) for which ^{77}Se NMR chemical shifts are known. The isotropic shielding tensor bears the following approximate relationship to the NMR chemical shift (eq 2)

$$\delta = \sigma_{\text{ref}} - \sigma_{\text{iso}} \quad (2)$$

where σ_{ref} is the isotropic shielding of an appropriate reference system. In ^{77}Se NMR spectroscopy, the chemical shifts are reported with respect to dimethyl selenide. As discussed previously,¹⁷ the average absolute error in all calculated chemical shifts is minimized by forming a linear regression line between the experimental chemical shift δ and the calculated isotropic shielding σ_{iso} (eq 3; see Figure 1S in the Supporting Information).

$$\delta = 1945.5 - 1.05\sigma_{\text{iso}} \quad (3)$$

The linear correlation coefficient is 0.996, indicating a good fit. Equation 3 has been utilized in the computation of the individual ^{77}Se chemical shifts of the molecular species.

The comparison of experimental and calculated ^{77}Se NMR chemical shifts is shown in Figure 5 and tabulated in Table 1S in Supporting Information. The line shown in Figure 5 is not a

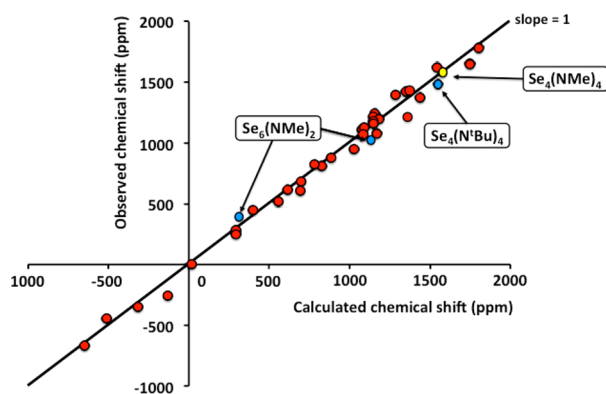


Figure 5. Observed and PBE0/def2-TZVPP-computed ^{77}Se chemical shifts of selenium-containing species. The red data points represent molecules for which the experimental ^{77}Se chemical shift is unambiguously known; the yellow data point is that of 1,3,5,7- $\text{Se}_4(\text{NMe})_4$ (**5b**), and the blue data points refer to 1,5- $\text{Se}_6(\text{NMe})_2$ (**1b**) and 1,3,5,7- $\text{Se}_4(\text{N}^t\text{Bu})_4$ (**5a**) (see text for these assignments).

linear regression line representing the data points. It portrays the ideal one-to-one correspondence between the computed and observed chemical shifts. A good agreement between calculated and experimental values can be seen in Figure 5, and a good performance of the PBE0 functional in the prediction of magnetic properties can be verified. (cf., ref 17).

The mean deviation between calculated and experimental chemical shifts is 46 ppm for the 32 different chemical shifts from 28 reference molecules shown in Supporting Information Table 1S. This is 10–30 ppm smaller than the values at the BP86, HF, and MP2 levels of theory.^{15b,31,32} It is well-known that the effect of different solvents on the ^{77}Se NMR chemical shift is on the order of 20–30 ppm. The computations of the chemical shifts, which have been performed on the individual molecules in vacuum, are close to the limit of accuracy that can be achieved. While more precise calculations could be obtained by taking solvent and relativistic effects into account,^{30,33} the experimental data have been recorded in several different solvents and produce imprecision in experimental values. The current approach to use optimized geometries and calculated shielding tensors in the gas phase also represents a compromise between precision and computational cost. However, it provides sufficient accuracy for the assignment of the experimental ^{77}Se NMR chemical shifts to new compounds.

As indicated in Figure 5 (yellow data point), the PBE0/def2-TZVPP-computed value of 1568 ppm for 1,3,5,7- $\text{Se}_4(\text{NMe})_4$ (**5b**) is in excellent agreement with the experimental ^{77}Se NMR chemical shift of 1585 ppm. The solution from which the crystals of 1,5- $\text{Se}_6(\text{NMe})_2 \cdot \frac{1}{2}\text{Se}_8$ (**1b**· $\frac{1}{2}\text{Se}_8$) were obtained showed several resonances in the ^{77}Se NMR spectrum of which those at 1028 and 399 ppm appeared in the intensity ratio 2:1. The PBE0/def2-TZVPP-computed ^{77}Se chemical shifts of **1b** are 1133 and 313 ppm (Figure 5). Although the agreement between the experimental and computed values is not as close as in the case of **5b**, it is within reasonable limits considering the accuracy of the computational method used in this work.

Identification of 1,3,5,7- $\text{Se}_4(\text{N}^t\text{Bu})_4$ (5a**).** On the basis of these computational results, it is now possible to assign the resonance at 1486 ppm, which was previously observed as the strongest signal in the complicated ^{77}Se NMR spectrum of the solution obtained by treating SeCl_2 with 3 equiv of $^t\text{BuNH}_2$.⁷ In this investigation, the latter reaction was repeated in different

molar ratios and monitored as a function of time. The changes in the composition of the products over time are illustrated in Figure 6 for the reaction of 1 equivalent of SeCl_2 with $2^{1/2}$ equiv of $^t\text{BuNH}_2$.

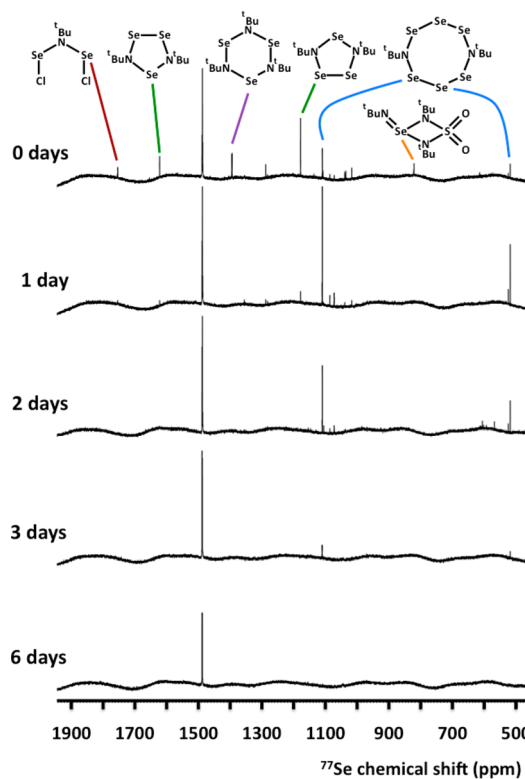


Figure 6. Development of the product distribution of a mixture of $^t\text{BuNH}_2$ and SeCl_2 (molar ratio $2^{1/2}$:1) in THF as a function of time.

When the molar ratio of the $^t\text{BuNH}_2$ and SeCl_2 was below 2:1, the main products are imidoselenium dichlorides $\text{ClSe}[\text{N}(^t\text{Bu})\text{Se}]_n\text{Cl}$ ($n = 1, 2$), as reported previously.⁹ With an increase of the relative amount of the amine above 2 equiv, the formation of cyclic selenium imides commences.⁷ For molar ratios in the range 2:1 to 3:1, the heterocycles 1,5- $\text{Se}_6(\text{N}^t\text{Bu})_2$ (**1a**), 1,3- $\text{Se}_3(\text{N}^t\text{Bu})_2$ (**3a**), and 1,3,5- $\text{Se}_3(\text{N}^t\text{Bu})_3$ (**4**) are the main products. The 15-membered ring 1,3,6,8,11,13- $\text{Se}_9(\text{N}^t\text{Bu})_6$ (**2**) is formed, when the molar ratio exceeds 3:1.⁷ As exemplified in Figure 6 for the $2^{1/2}$:1 reaction in THF, the composition of the mixture of products in solution becomes simpler over a period of several days with the concomitant formation of a red precipitate. After 1 day, only the unidentified 1486 ppm species⁷ and the resonances at 1111 and 521 ppm assigned to **1a**⁷ are observed. Upon further standing, the intensity of the latter resonances decreases, and these signals eventually disappear due to the crystallization of **1a** from the solution; only the resonance at 1486 ppm is apparent after 6 days. The $^{13}\text{C}\{^1\text{H}\}$ NMR spectrum of this solution showed two resonances at 59.2 ppm [$-\text{C}(\text{CH}_3)_3$] and 29.6 ppm [$-\text{C}(\text{CH}_3)_3$]. Thus, the NMR spectroscopic information indicates that all selenium atoms and all N^tBu groups are equivalent in the 1486 ppm species, which has been tentatively identified as 1,3,5,7- $\text{Se}_4(\text{N}^t\text{Bu})_4$ (**5a**).^{11,12} The PBE0/def2-TZVPP-computed chemical shift for **5a** of 1543 ppm (Figure 5) provides a reasonable confirmation of this assignment. Unfortunately, despite numerous attempts, this species showed no inclination to crystallize from THF solutions.

CONCLUSIONS

The cyclocondensation reaction of SeCl_2 with $(\text{Me}_3\text{Si})_2\text{NMe}$ provides a new approach to the synthesis of cyclic selenium imides which, unlike previous methods, predominantly generates a single product, i.e., the novel eight-membered ring 1,3,5,7- $\text{Se}_4(\text{NMe})_4$ (**5b**). This high-yielding synthesis opens the possibility of extensive investigations of the chemistry, especially the coordination behavior of this heterocycle. In addition, this new methodology has the potential to be applied to the clean syntheses of other cyclic chalcogen imides. For instance, all current methods for the preparation of *N*-alkyl substituted cyclic sulfur imides give a complex mixture of products.^{1,4b} The $(\text{Me}_3\text{Si})_2\text{NMe}$ reagent may also expand imidotellurium chemistry. To date, the only known cyclic tellurium imide is 1,3,5- $\text{Te}_3(\text{N}^t\text{Bu})_3$.³⁷

A detailed reinvestigation of the reaction of $t\text{BuNH}_2$ and SeCl_2 in THF showed that, at a molar ratio of $2^{1/2}:1$, the only selenium-containing product in solution after 3 days exhibits a resonance at 1486 ppm in the ^{77}Se NMR spectrum. On the basis of PBE0/def2-TZVPP calculations of ^{77}Se chemical shifts for a large selection of related selenium compounds, this resonance could be assigned to 1,3,5,7- $\text{Se}_4(\text{N}^t\text{Bu})_4$ (**5a**). These computations also provided the assignments of the two resonances for 1,5- $\text{Se}_6(\text{NMe})_2$ (**1b**), which was isolated in small amounts as the adduct $\text{1b}^{1/2}\text{Se}_8$ from the cyclocondensation reaction of SeCl_2 with $(\text{Me}_3\text{Si})_2\text{NMe}$. In the future, the good correlation between the experimental and computed ^{77}Se chemical shifts could turn out to be useful for confirming the identity of new cyclic selenium imides.

ASSOCIATED CONTENT

Supporting Information

X-ray crystallographic files of **5b** and $\text{1b}^{1/2}\text{Se}_8$ in CIF format. Selected bond parameters of **5b** and $\text{1b}^{1/2}\text{Se}_8$. Linear regression of the PBE0/def2-TZVPP calculated ^{77}Se isotropic shielding tensors and the experimental ^{77}Se chemical shifts. Cartesian coordinates of the PBE0/def2-TZVPP optimized geometries of **5b** and **1b**, as well as the 28 selenium compounds, which have been used in the shielding tensor calculations. The Supporting Information is available free of charge on the ACS Publications website at DOI: 10.1021/acs.inorgchem.5b00582.

AUTHOR INFORMATION

Corresponding Author

*E-mail: risto.laitinen@oulu.fi. Phone: +358294 481611.

Notes

The authors declare no competing financial interest.

ACKNOWLEDGMENTS

Financial support from Academy of Finland, Finnish Cultural Foundation, and Magnus Ehrnrooth Foundation (to A.J.K.) is gratefully acknowledged. T.C. is grateful to NSERC (Canada) for continuing funding. We are also grateful to Finnish CSC-IT Center for Science Ltd. for their generous provision of computational resources.

REFERENCES

(1) (a) Chivers, T. *A Guide to Chalcogen-Nitrogen Chemistry*; World Scientific Publishing Co. Pte. Ltd.: Singapore, 2005. (b) Chivers, T.; Laitinen, R. S. Chalcogen-Nitrogen Chemistry. In *Handbook of Chalcogen Chemistry, New Perspectives in Sulfur, Selenium and Tellurium*;

Devillanova, F., Ed.; RSC Press: Cambridge, U.K., 2007; pp 223–285. (c) Chivers, T.; Laitinen, R. S. Recent Developments in Chalcogen-Nitrogen Chemistry. *Handbook of Chalcogen Chemistry: New Perspectives in Sulfur, Selenium and Tellurium*; In Devillanova, F., du Mont, W.-W., Eds.; RSC Publishing: Cambridge, U.K., 2013; pp 191–237. (d) For a fascinating account of the history of cyclic sulfur imides, see: Heal, H. G. *The Inorganic Heterocyclic Chemistry of Sulfur, Nitrogen and Phosphorus*; Academic Press Inc. Ltd.: London, 1980; pp 16–40.

(2) (a) Lund, E. W.; Svendsen, S. R. *Acta Chem. Scand.* **1957**, *11*, 940–944. (b) Gregson, D.; Klebe, G.; Fuess, H. *J. Am. Chem. Soc.* **1988**, *110*, 8488–8493.

(3) (a) Hursthouse, M. B.; Malik, K. M. A.; Nabi, S. N. *J. Chem. Soc., Dalton Trans.* **1980**, 355–359. (b) Schmid, G.; Greese, R.; Boese, T. *Z. Naturforsch.* **1982**, *37B*, 620–626.

(4) (a) Jones, R.; Williams, D. J.; Woollins, J. D. *Angew. Chem., Int. Ed.* **1985**, *24*, 760–761. (b) Stone, B. B.; Nielsen, M. L. *J. Am. Chem. Soc.* **1959**, *81*, 3580–3584.

(5) Roesky, H. W.; Weber, K.-L.; Bats, J. W. *Chem. Ber.* **1984**, *117*, 2686–2692.

(6) Herberhold, M.; Jellen, W. *Z. Naturforsch.* **1986**, *41b*, 144–148.

(7) Maaninen, T.; Chivers, T.; Laitinen, R.; Schatte, G.; Nissinen, M. *Inorg. Chem.* **2000**, *39*, 5341–5347.

(8) Maaninen, A.; Chivers, T.; Parvez, M.; Pietikäinen, J.; Laitinen, R. *S. Inorg. Chem.* **1999**, *38*, 4093–4097.

(9) Maaninen, T.; Chivers, T.; Laitinen, R.; Wegelius, E. *Chem. Commun.* **2000**, 759–760.

(10) Maaninen, T.; Tuononen, H. M.; Schatte, G.; Suontamo, R.; Valkonen, J.; Laitinen, R.; Chivers, T. *Inorg. Chem.* **2004**, *43*, 2097–2104.

(11) Risto, M.; Eironen, A.; Männistö, E.; Oilunkaniemi, R.; Laitinen, R. S.; Chivers, T. *Dalton Trans.* **2009**, 8473–8475.

(12) Laitinen, R. S.; Oilunkaniemi, R.; Chivers, T., Synthesis, Structures, Bonding, and Reactions of Imido-Selenium and -Tellurium Compounds. In Woollins, J. D., Laitinen, R. S., Eds.; *Selenium and Tellurium Chemistry: From Small Molecules to Biomolecules and Materials*; Springer Verlag: Berlin, 2011; pp 103–122.

(13) Burns, R. C.; Collins, M. J.; Gillespie, R. J.; Schrobilgen, G. J. *Inorg. Chem.* **1986**, *25*, 4465–4469.

(14) Sheldrick, G. M. *Acta Crystallogr.* **2008**, *64A*, 112–120.

(15) (a) Nakanishi, W.; Hayashi, S. *J. Phys. Chem. A* **1999**, *103*, 6074–6081. and references therein. (b) Schreckenbach, G.; Ruiz-Morales, Y.; Ziegler, T. *J. Chem. Phys.* **1996**, *104*, 8605–8612 and references therein. (c) Laitinen, R.; Pakkanen, T. *J. Chem. Soc., Chem. Commun.* **1986**, 1381–1382. (d) Laitinen, R. S.; Pakkanen, T. *Inorg. Chem.* **1987**, *26*, 2598–2603. (e) Wrackmeyer, B.; Distler, B.; Gerstmann, M.; Herberhold, M. *Z. Naturforsch.* **1993**, *48b*, 1307–1314. (f) Maaninen, T.; Laitinen, R.; Chivers, T. *Chem. Commun.* **2002**, 1812–1813.

(16) (a) Perdew, J. P.; Burke, K.; Ernzerhof, M. *Phys. Rev. Lett.* **1996**, *77*, 3865–3868. (b) Perdew, J. P.; Ernzerhof, M.; Burke, K. *J. Chem. Phys.* **1996**, *105*, 9982–9985. Perdew, J. P.; Burke, K.; Ernzerhof, M. *Phys. Rev. Lett.* **1997**, *78*, 1396. (c) Adamo, C.; Barone, V. *J. Chem. Phys.* **1999**, *110*, 6158–6170.

(17) Maaninen, T.; Tuononen, H. M.; Kosunen, K.; Oilunkaniemi, R.; Hiitola, J.; Laitinen, R.; Chivers, T. *Z. Anorg. Allg. Chem.* **2004**, *630*, 1947–1954.

(18) Grimme, S.; Ehrlich, S.; Goerigk, L. *J. Comput. Chem.* **2011**, *32*, 1456–1465.

(19) Weigend, F.; Ahlrichs, R. *Phys. Chem. Chem. Phys.* **2005**, *7*, 3297–3305.

(20) (a) Björgvinnsson, M.; Roesky, H. W.; Pauer, F.; Stalke, D.; Sheldrick, G. M. *Inorg. Chem.* **1990**, *29*, 5140–5143. (b) Godfrey, S. M.; McAuliffe, C. A.; Pritchard, R. G.; Sarwar, S. *J. Chem. Soc., Dalton Trans.* **1997**, 1031–1035. (c) Maaninen, A.; Konu, J.; Laitinen, R. S.; Chivers, T.; Schatte, G.; Pietikäinen, J.; Ahlgrén, M. *Inorg. Chem.* **2001**, *40*, 3539–3543. (d) Mundt, O.; Becker, G.; Baumgarten, B.; Riffel, H.; Simon, A. *Z. Anorg. Allg. Chem.* **2006**, *632*, 1687–1709.

(21) (a) London, F. J. *Phys. Radium* **1937**, *8*, 397. (b) McWeeny, R. *Phys. Rev.* **1962**, *126*, 1028–1034. (c) Ditchfield, R. *Mol. Phys.* **1974**, *27*, 789–807. (d) Wolinski, K.; Hilton, J. F.; Pulay, P. *J. Am. Chem. Soc.* **1990**, *112*, 8251–8260. (e) Cheeseman, J. R.; Trucks, G. W.; Keith, T. A.; Frisch, M. J. *J. Chem. Phys.* **1996**, *104*, 5497–5509.

(22) Frisch, M. J.; Trucks, G. W.; Schlegel, H. B.; Scuseria, G. E.; Robb, M. A.; Cheeseman, J. R.; Scalmani, G.; Barone, V.; Mennucci, B.; Petersson, G. A.; Nakatsuji, H.; Caricato, M.; Li, X.; Hratchian, H. P.; Izmaylov, A. F.; Bloino, J.; Zheng, G.; Sonnenberg, J. L.; Hada, M.; Ehara, M.; Toyota, K.; Fukuda, R.; Hasegawa, J.; Ishida, M.; Nakajima, T.; Honda, Y.; Kitao, O.; Nakai, H.; Vreven, T.; Montgomery, J. A., Jr.; Peralta, J. E.; Ogliaro, F.; Bearpark, M.; Heyd, J. J.; Brothers, E.; Kudin, K. N.; Staroverov, V. N.; Kobayashi, R.; Normand, J.; Raghavachari, K.; Rendell, A.; Burant, J. C.; Iyengar, S. S.; Tomasi, J.; Cossi, M.; Rega, N.; Millam, M. J.; Klene, M.; Knox, J. E.; Cross, J. B.; Bakken, V.; Adamo, C.; Jaramillo, J.; Gomperts, R.; Stratmann, R. E.; Yazyev, O.; Austin, A. J.; Cammi, R.; Pomelli, C.; Ochterski, J. W.; Martin, R. L.; Morokuma, K.; Zakrzewski, V. G.; Voth, G. A.; Salvador, P.; Dannenberg, J. J.; Dapprich, S.; Daniels, A. D.; Farkas, Ö.; Foresman, J. B.; Ortiz, J. V.; Cioslowski, J.; Fox, D. J. *Gaussian 09, Revision D.01*; Gaussian, Inc.: Wallingford, CT, 2009.

(23) Zeiss, W.; Barlos, K. Z. *Naturforsch.* **1979**, *34B*, 423–425.

(24) (a) MacDonald, A. L.; Trotter, J. *Can. J. Chem.* **1973**, *51*, 2504–2506. (b) Esteban-Calderon, C.; Martinez-Ripoll, M.; Garcia-Blanco, S.; Vegas, A.; Garcia-Fernandez, H. *An. Quim., Ser. B* **1983**, *79*, 491–496.

(25) (a) Gasperin, M.; Freymann, R.; Garcia-Fernandez, H. *Acta Crystallogr., Sect. B* **1982**, *38*, 1728–1731. (b) Garcia-Fernandez, H.; Gasperin, M.; Freymann, R. *C. R. Acad. Sci., Ser. C* **1982**, *295*, 1109–1112.

(26) (a) Foss, O.; Janickis, J. V. *J. Chem. Soc., Dalton Trans.* **1980**, 624–627. (b) Maaninen, T.; Konu, J.; Laitinen, R. S. *Acta Crystallogr., Sect. E* **2004**, *60*, o2235–o2237.

(27) Emsley, J. *The Elements*, 3rd ed.; Clarendon Press: Oxford, 1998; p 292.

(28) The difference in energy is, however, virtually negligible.

(29) The optimized endocyclic PBE0/def2-TZVPP bond parameters of $\text{Se}_3(\text{NAd})_2$ ($r_{\text{SeSe}} = 2.385 \text{ \AA}$; $r_{\text{NSe}} = 1.831, 1.881 \text{ \AA}$; $\angle \text{NSeN} = 104.7^\circ$; $\angle \text{SeNSe} = 110.6^\circ$; and $\angle \text{NSeSe} = 92.6^\circ$; molecular symmetry C_2) agree well with those of the calculated parameters of 1,3- $\text{Se}_3(\text{N}^t\text{Bu})_2$ (**3a**) and with the experimental values from the crystal structure determination¹⁰ (see Figure 4).

(30) Nakanishi, W.; Hayashi, S. In *Organoselenium Chemistry between Synthesis and Biochemistry*; Santi, C., Ed.; Bentham Science Publishers: Sharjah, United Arab Emirates, 2014; pp 379–417.

(31) Bühl, M.; Thiel, W.; Fleischer, U.; Kutzelnigg, W. *J. Phys. Chem.* **1995**, *99*, 4000–4007 and references therein.

(32) It should be noted, however, that the previously reported mean deviations have been obtained using a much smaller set of selenium compounds and are therefore not strictly comparable with the present values.

(33) We have recently shown for a series of $\text{Se}_n\text{I}_m^{m+}$ ions³⁴ that the reliability of the prediction of ^{77}Se chemical shifts significantly improves by the use of ZORA (zeroth order regular approximation),³⁵ as well as the COSMO model (conductor-like screening model).³⁶ The inclusion of explicit molecules of the first solvation shell has been shown to be necessary in addition to continuum solvation effects.³⁵ This is exemplified by the SeI_3^+ ion:³⁴ The observed chemical shift is 830 ppm. Nonrelativistic vacuum value of the chemical shift is 1362 ppm. The ZORA vacuum chemical shift is 1294 ppm. The application of COSMO together with inclusion of one or more explicit solvent molecules in appropriate optimum locations increases the agreement (1 solvent molecule, 1133 ppm; 3 solvent molecules, 1006 ppm, 9 solvent molecules, 1004 ppm). The agreement in this case is still rather poor owing to the presence of very heavy iodine atoms in the ions.³⁴

(34) Brownridge, S.; Calhoun, L.; Jenkins, H. D. B.; Laitinen, R. S.; Murchie, M. P.; Passmore, J.; Pietikäinen, J.; Rautiainen, J. M.; Sanders, J. C. P.; Schrobilgen, G. J.; Suontamo, R. J.; Tuononen, H. M.; Valkonen, J. U.; Wong, C.-M. *Inorg. Chem.* **2009**, *48*, 1938–1959.

(35) Wolff, S. K.; Ziegler, T.; van Lenthe, E.; Baerends, E. J. *J. Chem. Phys.* **1999**, *110*, 7689–7698.

(36) (a) Klamt, A.; Jones, V. *J. Chem. Phys.* **1996**, *105*, 9972–9981. (b) Klamt, A. *J. Phys. Chem.* **1995**, *99*, 2224–2235. (c) Klamt, A.; Schüürmann, G. *J. Chem. Soc., Perkin Trans. 2* **1993**, 799–805.

(37) Chivers, T.; Gao, X.; Parvez, M. *J. Am. Chem. Soc.* **1995**, *117*, 2359–2360.